International Journal of Minerals, Metallurgy and Materials
Volume 21, Number 12, December 2014, Page 1233
DOI: 10.1007/s12613-014-1032-4

Preparation and characterization of regenerated MgO–CaO refractory bricks sintered under different atmospheres

Gui-bo Qiu[1)], *Chang-sheng Yue*[2)], *Xiang Li*[1)], *Min Guo*[1)], *and Mei Zhang*[1)]

1) Beijing Key Lab of Green Recycling and Extraction of Metals, School of Metallurgical and Ecological Engineering, University of Science and Technology Beijing, Beijing 100083, China

2) Central Research Institute of Building and Construction Co., Ltd., Metallurgical Corporation of China Ltd., Beijing 100088, China

(Received: 19 May 2014; revised: 7 July 2014; accepted: 8 July 2014)

Abstract: Regenerated MgO–CaO brick samples containing 80wt%, 70wt%, and 60wt% MgO were prepared using spent MgO–CaO bricks and fused magnesia as raw materials and paraffin as a binder. The bricks were sintered at 1873 K for 2 h under an air atmosphere and under an isolating system. The microstructure, mechanical properties at room temperature, and hydration resistance of the regenerated samples were measured and compared. The results indicated that the isolating sintering generated a strongly reducing atmosphere as a result of the incomplete combustion of paraffin, and the partial oxygen pressure was approximately 6.68×10^{-7} Pa. The properties of the regenerated bricks sintered under air conditions were all higher than those of the bricks sintered under a reducing atmosphere. The deterioration of the bricks was a result of MgO reduction and a decrease in the amount of liquid phase formed during sintering under a reducing atmosphere.

Keywords: refractories; regeneration; sintering atmospheres; mechanical properties; hydration

1. Introduction

MgO–CaO bricks are high-value refractories composed of lime (CaO) and periclase (MgO). They are widely used as lining bricks in refining furnaces [1] such as argon oxygen decarburization (AOD) furnaces used in the metallurgy industry because of their excellent properties of high temperature resistance, steel melt purification [2–3], etc. However, the broad application of MgO–CaO bricks is restricted by their strong tendency to hydrate [4]. The total consumption of MgO–CaO bricks in China was approximately 2.5×10^5 t in 2007 [5], resulting in an increasing amount of spent MgO–CaO bricks that have not been reutilized. These spent bricks not only occupy a substantial land area, but also waste valuable resources [6] such as MgO and CaO. The development of process that allows reuse of spent MgO–CaO bricks is urgently needed; however, the literature contains few studies on the reutilization of spent MgO–CaO bricks. Spent bricks have been used as refractory raw materials [5] and dry materials [7]; however, the maximum utilization of spent bricks used as raw materials was merely 25wt%, and only the parts of spent bricks that contained fewer impurities were made into dry materials because the spent bricks contained numerous impurities, including Fe_2O_3 and Al_2O_3 [8]; such impurities can significantly degrade the refractoriness [9] of regenerated products.

At present, heavy hazardous chrome bricks have been widely used in the firing zone of cement rotary kilns [10], especially in China [11]. Because of environmental concerns, many countries have passed legislation forbidding the use of chrome bricks [12]. Hence, the development of chrome-free refractory materials to replace chrome bricks is necessary. Because the operating temperature (approximately 1723 K) in a cement rotary kiln is lower than that in an AOD furnace (greater than 1923 K), regenerated MgO–CaO bricks can be reutilized in a cement rotary kiln; furthermore, MgO–CaO bricks exhibit excellent adhering coating properties [13], which is also a benefit of their application. Therefore, regenerated MgO–CaO bricks are expected to be recycled in a cement rotary kiln as a substitute for chrome bricks. This substitution would not only prevent chrome bricks from polluting the environment, but also enable the reuse of

Corresponding author: Mei Zhang E-mail: zhangmei@ustb.edu.cn

valuable resources in spent MgO–CaO bricks.

In our preliminary work, we successfully regenerated MgO–CaO bricks using spent MgO–CaO bricks from an AOD furnace and fused magnesia as raw materials at 1873 K for 2 h. The utilization of spent bricks in regenerated bricks was 67wt%, and the flexural strength at 1373 K was 60.81 MPa [8], which demonstrates the superior properties of the regenerated bricks. However, the properties of bricks regenerated using the same composition and synthesis process, with the exception of differences in the hermetic degree of the furnace, suggested that the sintering atmosphere may be the key point.

In this work, the regenerated MgO–CaO brick samples were prepared under normal air (oxidizing atmosphere) and isolating air (anoxic atmosphere) conditions. The phases, microstructure, mechanical properties at room temperature, and hydration resistance of regenerated MgO–CaO brick samples were investigated and compared.

2. Experimental

2.1. Materials

Regenerated MgO–CaO brick samples were prepared using spent MgO–CaO bricks and fused magnesia as raw materials and paraffin as a binder. The preparation procedure of green bodies containing 80wt%, 70wt%, and 60wt% MgO (hereafter referred to as M80, M70, and M60, respectively) is detailed elsewhere [8]. The size of the green bodies was 60 mm × 8 mm × 8 mm. Green bodies were separated into two groups: one group was sintered at 1873 K for 2 h as normal air was continuously bubbled into the furnace, whereas the other group was sintered in an isolating furnace. The compositions of the green bodies are shown in Table 1.

Table 1. Compositions of the green bodies

Samples	Mass fraction / %					Utilization ratio of spent MgO–CaO bricks / wt%
	MgO	CaO	Fe_2O_3	SiO_2	Al_2O_3	
Spent bricks	58.24	34.68	2.09	3.11	1.32	—
Fused magnesia	93.85	2.73	0.51	2.39	0.23	—
M80-a, M80-b*	80.00	15.16	1.12	2.67	0.65	38.89
M70-a, M70-b*	70.00	24.13	1.57	2.87	0.96	66.97
M60-a, M60-b*	60.00	33.10	2.01	3.07	1.27	95.06

Note: * Samples denoted as "a" were sintered under normal air; samples denoted as "b" were sintered under isolating air.

2.2. Test methods

The phases of regenerated MgO–CaO brick samples were analyzed by X-ray powder diffraction (XRD). The microstructure and elemental composition of the regenerated samples were detected by scanning electron microscopy (SEM) on a ZEISS OURIGR microscope equipped with an energy-dispersive X-ray spectrometer. Flexural and compression strengths at room temperature were measured using a WDW-10E microcomputer controlled electron universal testing machine.

Hydration resistance was tested via hot-water experiments in which the regenerated samples were first boiled in deionized water at 373 K for 1 h and then dried at 383 K for 24 h; the mass gain rate was subsequently measured. The mass gain rate was calculated by the follow equation:

$$\eta = \frac{W - W_1 - W_0}{W_0} \times 100\% \quad (1)$$

where η is the mass gain rate of the regenerated sample; W is the total mass of the regenerated sample and container after the experiment, g; W_0 is the mass of the regenerated sample before the experiment, g; and W_1 is the mass of the container, g. The mass gain rate was used to characterize the hydration resistance of the regenerated sample.

3. Results

3.1. Phases and microstructure of regenerated MgO–CaO bricks

Fig. 1 shows the XRD patterns of the regenerated samples that were sintered under conditions of normal air (Fig. 1(a)) and isolating air (Fig. 1(b)). As evident in the figure, the main phases of both regenerated samples are approximately the same, irrespective of the atmosphere. The main phases consist of MgO, CaO, and a small amount of Ca_3SiO_5. Besides, the character diffraction peaks of $Ca_2(AlFe)O_5$ (abbreviated as C_4AF) appeared only in samples M70 and M60 because of their greater impurity contents (Fe_2O_3 and Al_2O_3) compared with that of sample M80, which was clearly shown in Table 1. According to Ref. [14], $Ca_2Fe_2O_5$ (abbreviated as C_2F) was also formed in all regenerated samples; however, the characteristic diffraction peaks of C_2F are not evident in Fig. 1 because it was present in trace amounts.

SEM images of the fractures of the regenerated samples are shown in Fig. 2. The microstructure of the sample, whether sintered under normal air or isolating air, clearly became denser as the content of MgO was decreased. These results are consistent with those related to the bulk density, as shown in Table 2. Because the amounts of impurities such as Fe_2O_3 and Al_2O_3 increased as the content of MgO decreased, the low-melting-point materials C_4AF (melting

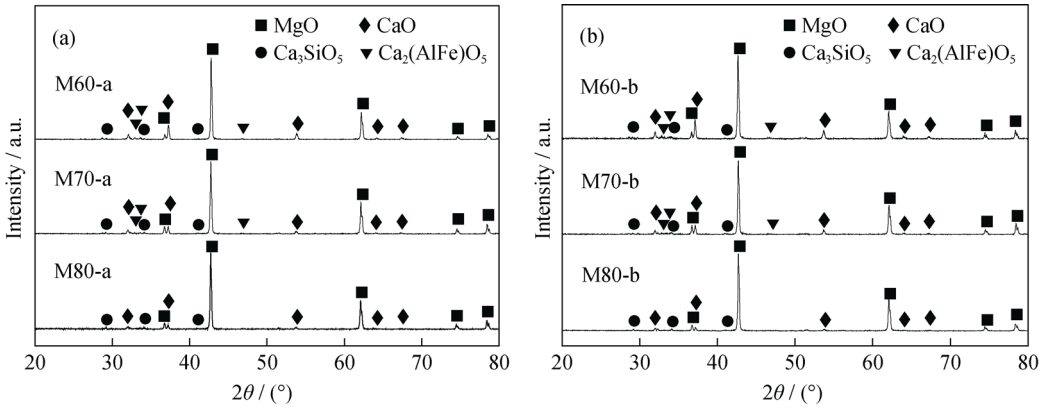

Fig. 1. XRD patterns of regenerated MgO–CaO brick samples sintered at 1873 K for 2 h: (a) sintered under normal air; (b) sintered under isolating air.

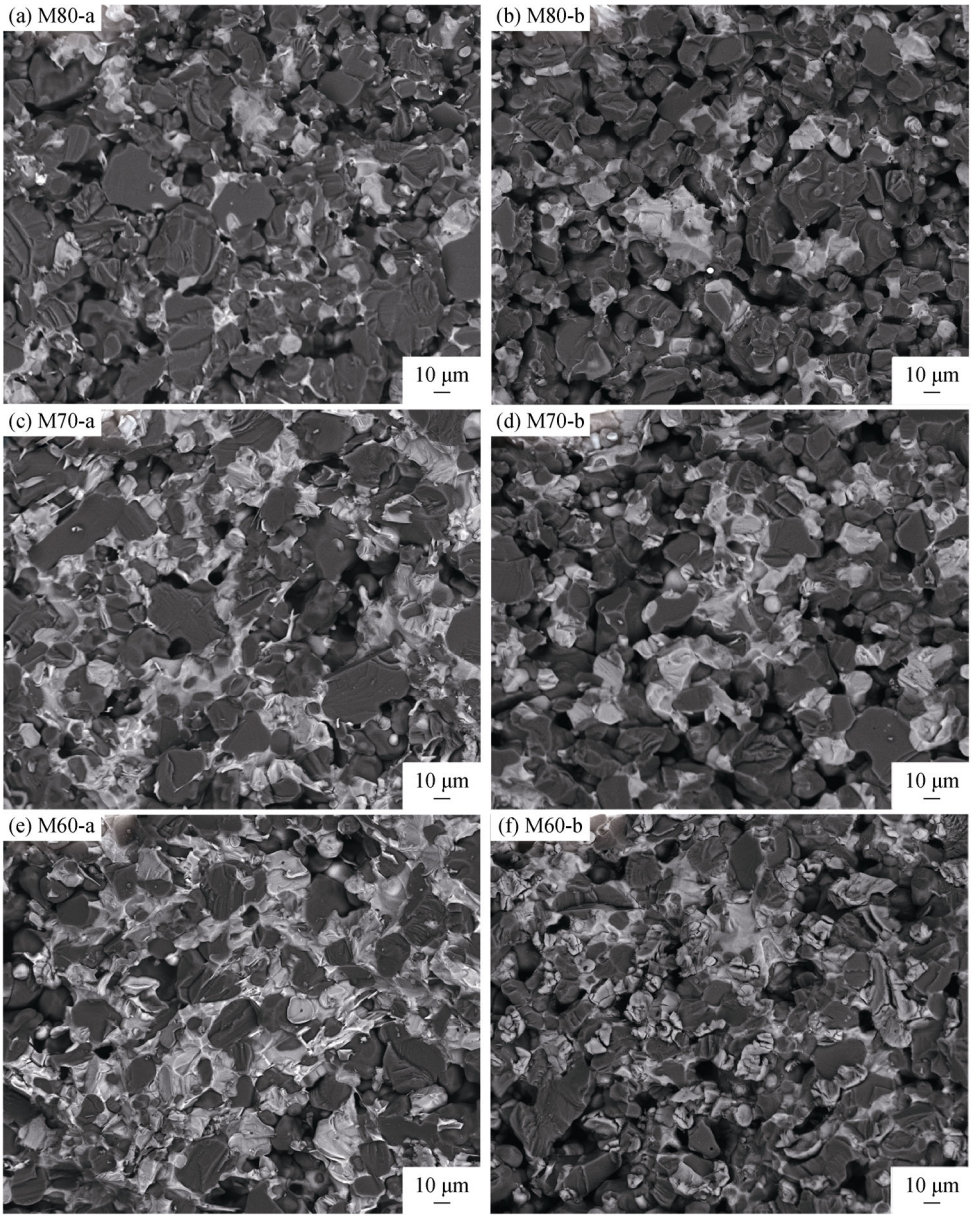

Fig. 2. Fracture SEM images of regenerated MgO–CaO brick samples sintered at 1873 K for 2 h: (a, c, and e) sintered under normal air; (b, d, and f) sintered under isolating air.

Table 2. Bulk density and mass gain rate of regenerated MgO–CaO brick samples

Sample No.	Bulk density / (g·cm^{-3})		Mass gain rate / %	
	a (Normal air)	b (Isolating air)	a (Normal air)	b (Isolating air)
M80	2.82	2.62	0.74	0.98
M70	2.95	2.72	0.84	1.40
M60	3.07	2.84	0.90	2.49

point of 1688 K [14]) and C_2F (melting point of 1722 K [14]) were gradually generated; the presence of these materials facilitated sintering. The bulk density was directly dependent on the sintering atmosphere; i.e., regenerated samples with a much greater density were obtained under normal air (Table 2), as clearly observed via a comparison of Fig. 2(a) with Fig. 2(b). These results indicate that a normal air sintering atmosphere could improve the bulk density of regenerated samples.

3.2. Mechanical properties measurements at room temperature

The flexural and compression strengths at room temperature of regenerated samples under different sintering atmospheres are shown in Fig. 3. As evident in the figure, the flexural and compression strengths were both enhanced with a decrease in MgO content. The minimum compression strengths of the regenerated samples sintered under isolating air and normal air conditions are 238.91 MPa and 251.37 MPa respectively, both of which represent improved the mechanical properties. In addition, the mechanical properties of the regenerated samples sintered under normal air were all better than those sintered under isolating air conditions, which was a consequence of the increase in bulk density, as shown in Table 2.

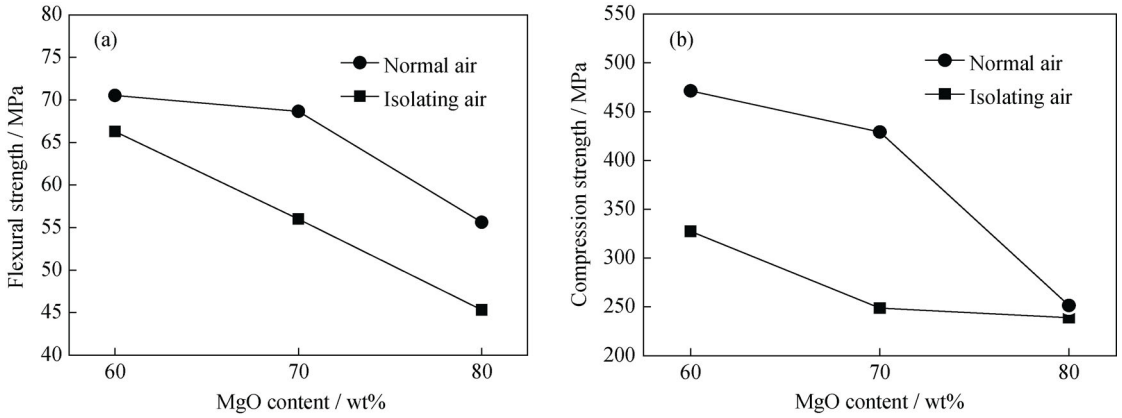

Fig. 3. Flexural strength (a) and compression strength (b) at room temperature of regenerated MgO–CaO brick samples sintered at 1873 K for 2 h.

3.3. Hydration resistance investigation

Hydration resistance is one of the key properties of MgO–CaO bricks and may reflect their stability during storage and transport. The mass gain rate of the regenerated samples after the hot-water experiments is also shown in Table 2. As evident from the results, the mass gain rate increased with decreasing MgO content. However, the mass gain rate of regenerated samples sintered under normal air was lower than that of samples sintered under isolating air condition. As shown in Table 2, the mass gain rate of sample M60-a sintered under normal air conditions was only 0.90%, which was even lower than that of sample M80-b sintered under isolating air conditions. Hence, the results illustrate that sintering under normal air conditions can also enhance the hydration resistance of the regenerated samples, which is similar to the results related to the bulk density and mechanical properties.

4. Discussion

4.1. Macroscopic observations of alumina crucibles after sintering under different atmospheres

Alumina crucibles were used to contain the regenerated samples. Significant differences in the inner walls of the alumina crucibles after sintering under normal air and those after sintering under isolating air are shown in Fig. 4. The inner wall of the alumina crucible sintered under normal air conditions was only slightly changed to yellow from white; no more other obvious changes were observed in Fig. 4(a). However, numerous white flocculent fibers were observed on the inner walls of alumina crucibles sintered under isolating air conditions, as shown in the image in the top corner of Fig. 4(b); the surface of the alumina crucible was simultaneously changed to black.

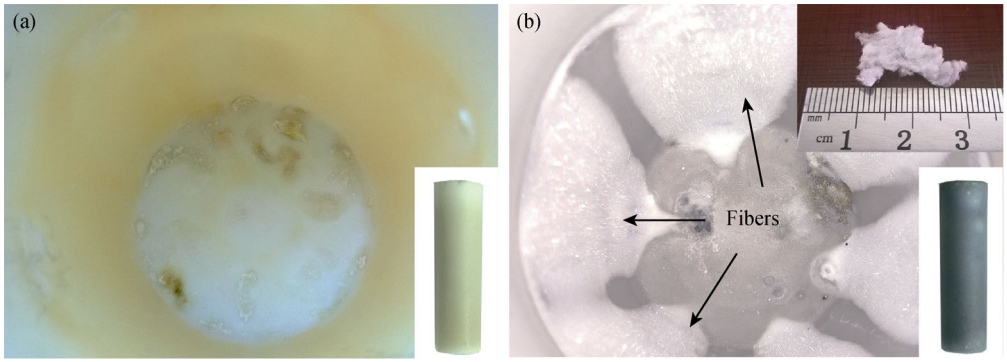

Fig. 4. Photographs of alumina crucible inner walls after sintering at 1873 K for 2 h: (a) crucible sintered under normal air (the inset is the picture of the crucible); (b) crucible sintered under isolating air (the top inset shows the white flocculent fibers and the corner inset shows a picture of the crucible).

4.2. Atmospheric analysis during isolating sintering

Macroscopic observation of alumina crucibles showed great differences after green bodies were sintered under normal air and isolating air conditions. In addition, a comparison of the properties of regenerated samples — specifically, the bulk density, mechanical properties at room temperature, and hydration resistance — indicated that the use of an air sintering atmosphere improved the properties of the regenerated samples.

During the sintering, only binder paraffin changed the atmosphere. Paraffin is a mixture of hydrocarbons with 22–36 carbon atoms. Therefore, it is prone to incomplete combustion in an anoxic system and tends to generate carbon black (C). Actually, carbon black was observed on the inner wall of the alumina crucibles used to contain the regenerated samples sintered under isolating air conditions (black region in Fig. 4(b)); however, it was not observed in samples sintered under normal air conditions (Fig. 4(a)). These results demonstrate that paraffin did not completely combust under the isolating air conditions and that the atmosphere was reductive because carbon black was present in excess. Thus, the atmosphere — specifically, the oxygen partial pressure in the sintering system — was responsible for the lack of complete combustion.

After the isolating air sintering process, some white flocculent fibers were deposited onto the inner wall of the alumina crucible. They were determined to be magnesium aluminate spinel ($MgAl_2O_4$), as shown in Fig. 5. In addition, the mass loss of MgO from the regenerated samples was also determined (Table 3). Compared with original MgO mass, that of the sample sintered under isolating air conditions was much lower. We considered that MgO may have been reduced to Mg(g) by carbon black (C) and that Mg (g) may have evaporated out and then deposited on the inner wall of the alumina crucible, where the oxygen partial pressure (P_{O_2}) was higher than that of nearby sample. As a consequence, Mg(g) was reoxidized to MgO and further reacted with alumina crucible, resulting in the formation of white flocculent fibers ($MgAl_2O_4$) on the inner wall of the alumina crucible. The observed results again demonstrated samples sintered under isolating air conditions were exposed to a strongly reducing atmosphere.

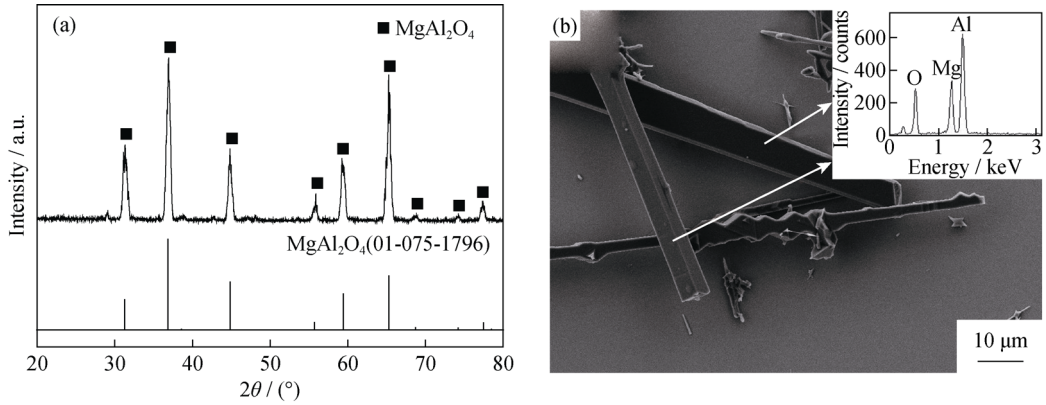

Fig. 5. XRD pattern (a) and SEM image (b) of flocculent fibers deposited onto the inner wall of the alumina crucible sintered under isolating air.

Table 3. Mass of MgO in regenerated sample M80 before and after sintering

Sample	Mass of MgO / g
Original	64.00
M80-a	63.95
M80-b	60.66

4.3. Partial oxygen pressure calculation in the isolating system

The equilibrium between MgO(s) and Mg(g) is shown as follows:

$$MgO(s) + C(s) = CO(g) + Mg(g) \quad (2)$$

$$\Delta_r G^{\ominus}_{(2)} = 613.27 - 0.29\,T, \text{ kJ/mol} \quad (1500–2000 \text{ K}) \text{ [15]}.$$

At 1873 K, the standard Gibbs free energy ($\Delta_r G^{\ominus}$) of Eq. (2) is 70.10 kJ/mol, which is positive. This standard Gibbs free energy indicates that MgO could not be reduced by C at 1873 K under standard conditions. However, if a strongly reducing atmosphere is present and the partial pressure of Mg(g) ($P_{Mg(g)}$) is sufficiently low, the reaction shown in Eq. (2) can occur at 1873 K, as directly evidenced by the mass loss of MgO in the regenerated samples (Table 3).

Here, sample M80-b sintered under isolating air conditions was selected as an example to calculate the oxygen partial pressure in the isolating furnace. The total mass loss of MgO was 3.34 g, as shown in Table 3. We assumed that all of the mass loss was associated with the reduction of MgO and CaO, and ignored the reductions of other impurities.

The amount of substance of CO (n_{CO}, mol) can be calculated from Eq. (2) with a known condition of m(MgO(s)) = 3.34 g, $n_{CO} = n_{MgO} = 8.35 \times 10^{-2}$ mol.

The pressure of CO (P_{CO}) can be calculated from the following equation:

$$P_{CO}V = n_{CO}RT \quad (3)$$

where P_{CO} is the pressure of CO, Pa; V is the gas volume of the isolating system, $V = 1.00 \times 10^{-4}$ m^3; n_{CO} is the amount of CO, mol; R is the ideal gas constant, $R = 8.314$ J/(mol·K); T is the temperature, $T = 1873$ K. Hence, $P_{CO} = 1.30 \times 10^7$ Pa.

The equilibrium between C(s) and CO(g) is shown as follows:

$$C(s) + 0.5O_2(g) = CO(g) \quad (4)$$

$$\Delta_r G^{\ominus}_{(4)} = -116.86 - 0.085\,T, \text{kJ/mol} \quad (1500–2000 \text{ K}) \text{ [15]}.$$

When the reaction shown in Eq. (4) reached thermodynamic equilibrium at 1873 K, $\Delta G^{\ominus}_{1873} =$ –276.07 kJ/mol.

The oxygen partial pressure (P_{O_2}) can be calculated by using the following equation:

$$\Delta G_T = \Delta G^{\ominus}_T + RT \ln \frac{P_{co}/p^{\ominus}}{(P_{O_2}/P^{\ominus})^{0.5}} \quad (5)$$

When the system is at thermodynamic equilibrium, $\Delta G_T = 0$. Substituting $T = 1873$ K, $P_{CO} = 1.30 \times 10^7$ Pa, $\Delta G^{\ominus}_T = -276.07$ kJ/mol, $P^{\ominus} = 1.01 \times 10^5$ Pa into Eq. (5), we obtain $P_{O_2} = 6.68 \times 10^{-7}$ Pa.

Therefore, we directly proved the strongly reductive sintering atmosphere in the isolating system.

4.4. Effect of sintering atmosphere on the regeneration of MgO–CaO bricks

Fig. 6 shows SEM images of the surface of M80 samples sintered under normal air (oxidizing system) and under isolating air conditions (reductive system). We observed that numerous white banding phases (area B in Fig. 6(b)) grew on the surface of MgO grains of sample M80-b (Fig. 6(b)); however, they were not observed in sample M80-a sintered under an oxidizing atmosphere (Fig. 6(a)). The elemental composition of the white banding phases and that of the area A in Fig. 6(a) as a comparison were analyzed by energy-dispersive X-ray spectroscopy (EDS); the results are shown in Table 4. The results indicate that, under reducing conditions, the MgO grains in sample M80-b accumulated substantially more Fe (as Fe(II) or Fe(III)). Fe(II) and Fe(III) tend to be soluble in the MgO crystal lattice at 1873 K; in addition, Fe(II) is completely soluble in MgO [16]. Because the atmosphere was reductive during the sintering under isolating air conditions, a portion of the Fe(III) was reduced to Fe(II). MgO could dissolve much more elemental Fe under a reducing atmosphere than under an oxidizing one. During the temperature-decreasing period after sintering, elemental Fe was precipitated from MgO crystals and reacted with CaO to form low-melting-point white banding materials.

Fe is one of the main components of C_4AF and C_2F, which form a liquid phase at 1873 K. During the sintering under reducing conditions, the content of C_4AF and C_2F decreased because of the substantial amount of Fe that dissolved into the MgO crystal lattice; thus, the amount of liquid phase formed from C_4AF and C_2F decreased during sintering, which inhibited the sintering process. Furthermore, the decrease in the amount of liquid phase resulted in decreased bulk density of the regenerated samples; as a result, the mechanical properties at room temperature and the hydration resistance of the samples decreased as well. In addition, the mass loss of MgO under a reducing atmosphere also contributed to the decrease of the bulk density of the regenerated samples.

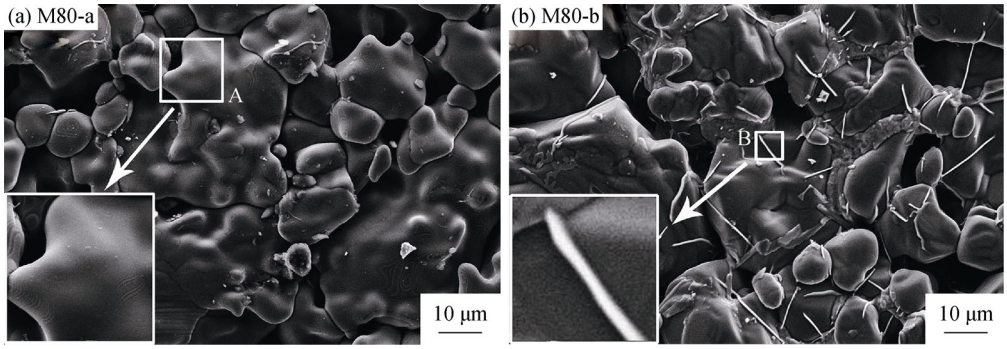

Fig. 6. SEM images of the surfaces of regenerated sample M80 sintered at 1873 K for 2 h under different atmospheres: (a) normal air; (b) isolating air.

Table 4. EDS analysis results of areas A and B in Fig. 6 for sample M80 sintered under normal air and under isolating air conditions at%

Area	O	Mg	Ca	Fe	Si	Al
A	49.14	50.44	0.32	0.10	—	—
B	55.29	40.00	2.36	2.06	0.14	0.15

5. Conclusions

Regenerated MgO–CaO brick samples were prepared using spent MgO–CaO bricks from AOD and fused magnesia as raw materials and were sintered under normal air and isolating air conditions. The bulk density, mechanical properties, and hydration resistance of the regenerated samples were investigated and compared. According to thermodynamic calculations, the P_{O_2} in the isolating air system for regenerated samples containing 80wt% MgO was as low as 6.68×10^{-7} Pa because of the incomplete combustion of paraffin. The results indicated that the isolating air system provided a strongly reducing atmosphere that caused the reduction of MgO and, consequently, a decrease in the bulk density of the sample. At the same time, the amount of Fe dissolved in the MgO crystal lattice increased, which resulted in diminished formation of the liquid phase from C_4AF and C_2F. The diminished amount of the liquid phase inhibited sintering. Hence, the bulk density, mechanical properties, and hydration resistance of the regenerated samples sintered under air conditions were all superior to that of the samples sintered under a reducing atmosphere.

Acknowledgements

This work was financially supported by the National Natural Science Foundation of China (Nos. 51372019, 51074009, and 50874013) and the National Science and Technology Supporting Program (No. 2011BAB03B02).

References

[1] H.I. Moorkah and M.S. Abolarin, Investigation of the properties of locally available dolomite for refractory application, *Niger. J. Technol.*, 24(2005), No. 1, p. 79.

[2] M. Soltanieh and Y. Payandeh, Relationship between oxygen chemical potential and steel cleanliness, *J. Iron Steel Res. Int.*, 12(2005), No. 5, p. 28.

[3] M. Rabah and E.M.M. Ewais, Multi-impregnating pitch-bonded Egyptian dolomite refractory brick for application in ladle furnaces, *Ceram. Int.*, 35(2009), No. 2, p. 813.

[4] F. Kashaninia, H. Sarpoolaky, R. Naghizadeh, A.R. Bagheri and M. Zamanipour, Improving hydration resistance of magnesia-doloma refractories by iron oxide addition, *Iran. J. Mater. Sci. Eng.,* 8(2011), No. 4, p. 34.

[5] Y.B. Liang and X.L. Shen, Effects of spent MgO–CaO bricks additive amount on the properties of baking MgO–CaO bricks, *Refractories*, 42(2008), No. 5, p. 392.

[6] S.M. Huang, Y. Yang, and Q.H. Xue, Research progress of recycling of used refractories, *Refractories*, 41(2007), No. 6, p. 460.

[7] W. Zhang, G. Shi, F.C. Wei, and C.Y. Wang, Preparation of magnesia–calcia dry mix from used MgO–CaO bricks, *Refractories*, 46(2012), No. 2, p. 126.

[8] G.B. Qiu, B. Peng, M. Guo, and M. Zhang, Regeneration utilization of spent MgO–CaO bricks for argon oxygen decarburization furnace, *J. Chin. Ceram. Soc.*, 41(2013), No. 9, p. 1284.

[9] A. Ghosh, T.K. Bhattacharya, B. Mukherjee, H.S. Tripathi, and S.K. Das, Effect of Fe_2O_3 on the densification and properties of lime, *Ceram. Silikaty*, 47(2003), No. 2, p. 70.

[10] S. Ghanbarnezhad, A. Nemati, M. Bavand-Vandchali, and R. Naghizadeh, New development of spinel bonded chrome-free basic brick, *J. Chem. Eng. Mater. Sci.,* 4(2013), No. 1, p. 7.

[11] W. Zhou, Y.H. Yue, H.R. Kang, Y.J. Li, and Y. Li, Develop-

ment and application of chrome free bricks for tall temperate zone of new dry process cement kiln, *China Cem.*, (2010), No. 11, p. 65.

[12] C.L. Macey, Refractory solutions for high wear in cement kiln transition zones, [in] 5*th Unified International Technical Conference on Refractories — a Worldwide Technology (UNITECR* 97*)*, New Orleans, LA, 1997, p. 1625.

[13] Z.Q. Guo, S. Palco, and M. Rigaud, Bonding of cement clinker onto doloma-based refractories, *J. Am. Ceram. Soc.,* 88(2005), No. 6, p. 1481.

[14] N. Li, H.Z. Gu, and H.Z. Zhao, *Refractory Materials Science*, Metallurgy Industry Press, Beijing, 2010, p. 198.

[15] B. Ihsan, *Thermochemical Data of Pure Substances*, Translated by N.L. Cheng, S.T. Niu, and G.Y. Xu, Science Press, Beijing, 2003.

[16] H. Aygül Yeprem, Effect of iron oxide addition on the hydration resistance and bulk density of doloma, *J. Eur. Ceram. Soc*., 27(2007), No. 2-3, p. 1651.